

Crystal Structure of $\text{Li}_2\text{B}_{12}\text{H}_{12}$: a Possible Intermediate Species in the Decomposition of LiBH_4

Jae-Hyuk Her,^{*,†,‡} Muhammed Yousufuddin,^{†,‡} Wei Zhou,^{†,‡} Satish S. Jalisatgi,[§] James G. Kulleck,^{||} Jason A. Zan,^{||} Son-Jong Hwang,[⊥] Robert C. Bowman, Jr.,^{||} and Terrence J. Udovic[†]

NIST Center for Neutron Research, National Institute of Standards and Technology, Gaithersburg, Maryland 20899, Department of Materials Science and Engineering, University of Maryland, College Park, Maryland 20742, International Institute of Nano and Molecular Medicine, Department of Radiology, University of Missouri, Columbia, Missouri 65211, Jet Propulsion Laboratory, California Institute of Technology, Pasadena, California 91109, and Division of Chemistry and Chemical Engineering, California Institute of Technology, Pasadena, California 91125

Received July 18, 2008

The crystal structure of solvent-free $\text{Li}_2\text{B}_{12}\text{H}_{12}$ has been determined by powder X-ray diffraction and confirmed by a combination of neutron vibrational spectroscopy and first-principles calculations. This compound is a possible intermediate in the dehydrogenation of LiBH_4 , and its structural characterization is crucial for understanding the decomposition and regeneration of LiBH_4 . Our results reveal that the structure of $\text{Li}_2\text{B}_{12}\text{H}_{12}$ differs from other known alkali-metal (K, Rb, and Cs) derivatives.

Lithium borohydride (LiBH_4) has garnered great interest recently as a potentially viable hydrogen-storage material. However, its stability requires high temperatures for decomposition and hydrogen release. Consequently, many studies involving destabilization have been performed to improve low-temperature reversibility. Recently, lithium dodecahydrododecaborate ($\text{Li}_2\text{B}_{12}\text{H}_{12}$) was suggested as an intermediate species in the decomposition process of LiBH_4 , based on theoretical calculations¹ and experimental results.^{2–4} Thus, a thorough study of $\text{Li}_2\text{B}_{12}\text{H}_{12}$ is needed

to better understand the decomposition process of LiBH_4 , thereby facilitating future studies into its destabilization.

The structures of other alkali-metal dodecahydrododecaborates ($\text{A}_2\text{B}_{12}\text{H}_{12}$, A = K, Rb, Cs) are already well-known.⁵ However, the lithium derivative has not been reported except in its heptahydrated form.⁶ Possible $\text{Li}_2\text{B}_{12}\text{H}_{12}$ structures have been proposed from calculations.¹ In this study, we have determined the crystal structure of $\text{Li}_2\text{B}_{12}\text{H}_{12}$ from powder X-ray diffraction (XRD). Moreover, we present first-principles calculations, which confirm the stability of this structure and are also in agreement with the phonon density of states (DOS) measured via neutron vibrational spectroscopy (NVS).

The synthesis of polycrystalline $\text{Li}_2\text{B}_{12}\text{H}_{12}$ is described in the literature.⁷ Because the material is extremely hygroscopic, we evacuated the sample at 473 K to ensure the anhydrous form. The resulting white powder was loaded into a thin-walled glass capillary under a He atmosphere and sealed with vacuum grease. The XRD pattern was collected at room temperature.

The diffraction pattern in Figure 1 was autoindexed as cubic, as reported in the literature,⁷ but in contrast to the anhydrous structures of other alkali-metal (i.e., K, Rb, and Cs) derivatives (space group $Fm\bar{3}$), the face-centering operation was not preserved, and a primitive unit cell was required. This structural difference is perhaps due to the much smaller radius of the Li^+ cation. (For example, the Pauling ionic radius of K^+ is 1.33 Å, while that of Li^+ is 0.60 Å.⁸) Systematic absences of Bragg reflections were consistent with $Pa\bar{3}$, a subgroup of $Fm\bar{3}$, and characterized with pseudo-

* To whom correspondence should be addressed. E-mail: jhher@nist.gov.

[†] National Institute of Standards and Technology.

[‡] University of Maryland.

[§] University of Missouri.

^{||} Jet Propulsion Laboratory, California Institute of Technology.

[⊥] Division of Chemistry and Chemical Engineering, California Institute of Technology.

(1) Ohba, N.; Miwa, K.; Aoki, M.; Noritake, T.; Towata, S.-I.; Nokamori, Y.; Orimo, S.-I.; Züttel, A. *Phys. Rev. B* **2006**, *74*, 075110.

(2) Orimo, S.-I.; Nakamori, Y.; Ohba, N.; Miwa, K.; Aoki, M.; Towata, S.-I.; Züttel, A. *Appl. Phys. Lett.* **2006**, *89*, 021920.

(3) Mosegaard, L.; Møller, B.; Jørgensen, J.-E.; Bösenberg, U.; Dornheim, M.; Hanson, J. C.; Cerenius, Y.; Walker, G.; Jakobsen, H. J.; Besenbacher, F.; Jensen, T. R. *J. Alloys Compd.* **2007**, *446–447*, 301.

(4) Hwang, S.-J.; Bowman, R. C.; Reiter, J. W.; Rijssenbeek, J.; Soloveichik, G. L.; Zhao, J.-C.; Kabbour, H.; Ahn, C. C. *J. Phys. Chem. C* **2008**, *112*, 3165.

(5) Tiritiris, I.; Schleid, T. *Z. Anorg. Allg. Chem.* **2003**, *629*, 1390.

(6) Tiritiris, I.; Schleid, T. *Z. Anorg. Allg. Chem.* **2002**, *628*, 1411.

(7) Johnson, J. W.; Brody, J. F. *J. Electrochem. Soc.* **1982**, *129*, 2213.

(8) Huheey, J. E.; Keiter, E. A.; Keiter, R. L. *Inorganic Chemistry: Principles of Structure and Reactivity*, 4th ed.; Harper Collins: New York, 1993.

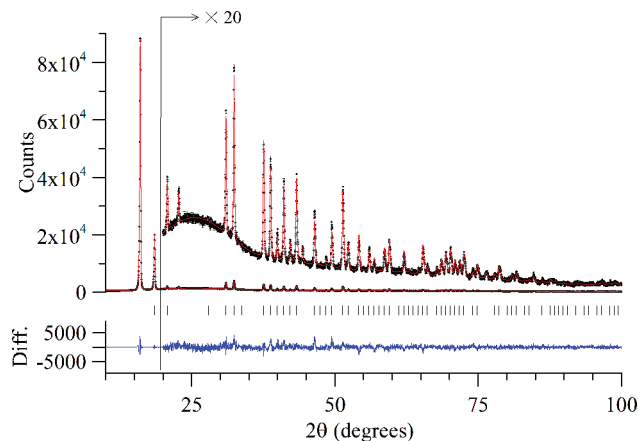


Figure 1. XRD pattern of anhydrous, crystalline $\text{Li}_2\text{B}_{12}\text{H}_{12}$ and the Rietveld refinement result. Black: raw data points. Red: calculated profile. Blue: difference curve (observed – calculated) on the same scale. Vertical tick marks: allowed Bragg reflection positions. After $2\theta \sim 24^\circ$, the additional pattern and difference curve are both presented with $20\times$ magnification.

face-centering symmetry operations. The structure was solved by a direct space searching (simulated annealing) method followed by full-profile Rietveld refinement using molecular-shaped constraints.

The $\text{Li}_2\text{B}_{12}\text{H}_{12}$ structure in Figure 2 can be understood as a rational variation of the face-centered K derivative. Because Li^+ is a significantly smaller cation, the unit cell dimensions are reduced by $\sim 9\%$ [$10.6290(8)$ Å for $\text{K}_2\text{B}_{12}\text{H}_{12}^{5-}$ to $9.5771(2)$ Å for $\text{Li}_2\text{B}_{12}\text{H}_{12}$] and a different internal symmetry is favored. In the case of $\text{K}_2\text{B}_{12}\text{H}_{12}$, the $\text{B}_{12}\text{H}_{12}^{2-}$ anion is surrounded by eight K^+ cations within the cubic geometry, while the K^+ cation is tetrahedrally surrounded by four $\text{B}_{12}\text{H}_{12}^{2-}$ anions with a $\text{K}-\text{H}$ distance of 2.94 Å.⁵ For $\text{Li}_2\text{B}_{12}\text{H}_{12}$, our refined structure reveals that the Li^+ cation is displaced $1.824(7)$ Å from the tetrahedral site. Instead, it lies on a near-trigonal-planar site formed by three $\text{B}_{12}\text{H}_{12}^{2-}$ anions, each of which resides in the octahedral cage defined by six Li^+ cations. Each $\text{B}_{12}\text{H}_{12}^{2-}$ anion orients two H atoms to each of the Li^+ cations, resulting in a strongly distorted octahedral coordination of the Li^+ cation with six H atoms. The observed $\text{H}-\text{Li}-\text{H}$ angles are $66.7(6)^\circ$, $91.9(7)^\circ$, $93.8(4)^\circ$, and $106.6(2)^\circ$. This arrangement seems to optimally satisfy Li^+ 's small ionic radius and short bond length to the H of $\text{B}_{12}\text{H}_{12}^{2-}$. The two unique $\text{Li}-\text{H}$ distances [$2.077(7)$ and $2.216(7)$ Å] are smaller compared to that of $\text{K}_2\text{B}_{12}\text{H}_{12}$. This significant change is attributed to the alternating orientations of the $\text{B}_{12}\text{H}_{12}^{2-}$ anions, which break the face-centering and reduce the symmetry to $Pa\bar{3}$, in addition to the lattice parameter contraction. The packing diagrams representing the trigonal planar and octahedral building blocks are given in Figure 3.

This structural behavior is reminiscent of the well-known crystalline C_{60} order–disorder phase transition,⁹ which shows rotational ordering below 249 K by lowering the symmetry from $Fm\bar{3}$ to $Pa\bar{3}$. Its transition was also explained by intermolecular electrostatic interactions inducing an optimal arrangement of C_{60} molecules.

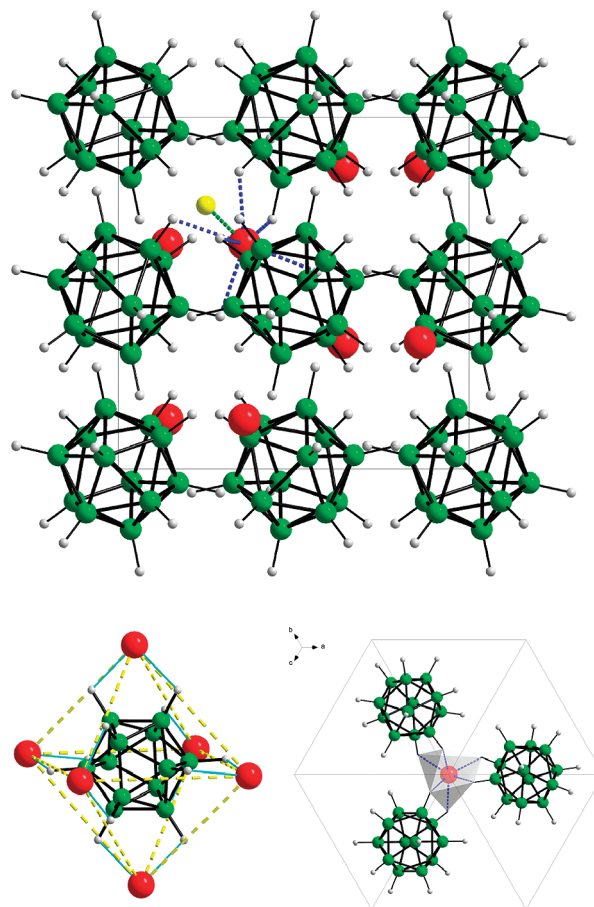


Figure 2. Structure of $\text{Li}_2\text{B}_{12}\text{H}_{12}$. (top) Unit cell view along the (100) direction. Blue dashed lines: $\text{Li}-\text{H}$. Green dashed line: Li tetrahedral site ($1/4, 1/4, 1/4$) of the face-centered cubic (fcc). Note that the $\text{B}_{12}\text{H}_{12}$ cages are not face-centered because of the respective orientations of the cages. The Li^+ cation position also deviates from the ideal tetrahedral site (represented by the yellow ball) to the near-trigonal-planar site along the body diagonal direction. (bottom left) Configuration of the six nearest Li^+ cations around the $\text{B}_{12}\text{H}_{12}^{2-}$ anion. Yellow dashed lines clarify the octahedral geometry, and thin solid light-blue lines represent $\text{Li}-\text{H}$ bond distances. (bottom right) Triangular arrangement of the $\text{B}_{12}\text{H}_{12}$ units surrounding a Li^+ cation. Li: red. B: green. H: silver.

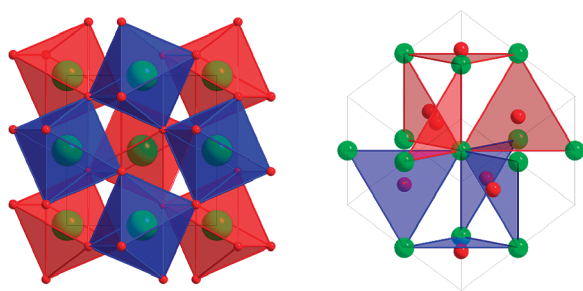


Figure 3. Packing diagram for $\text{Li}_2\text{B}_{12}\text{H}_{12}$. Green ball: center position of the $\text{B}_{12}\text{H}_{12}^{2-}$ anion. Red ball: Li . (left) $\text{B}_{12}\text{H}_{12} + 6 \text{Li}$ are represented by octahedra. Note that their corners are shared by three octahedra instead of two, the usual corner-sharing scheme of octahedra, as in the perovskite structure. (right) Triangles represent the three $\text{B}_{12}\text{H}_{12}^{2-}$ anions nearest each Li^+ cation. Li^+ is almost at the center of the triangular plane. The colors for the polyhedra are used for clarification. All $[\text{B}_{12}\text{H}_{12}]^{2-}$ and Li^+ ions are crystallographically equivalent.

Ohba et al.¹ theoretically predicted a $\text{Li}_2\text{B}_{12}\text{H}_{12}$ structure with similar geometry but in a monoclinic cell. In order to confirm the stability of our refined structure, we performed first-principles calculations within the plane-wave implementation of the generalized gradient approximation to

(9) David, W. I. F.; Ibberson, R. M.; Matthewman, J. C.; Prassides, K.; Dennis, T. J. S.; Hare, J. P.; Kroto, H. W.; Taylor, R.; Walton, D. R. M. *Nature* **1991**, *353*, 147.

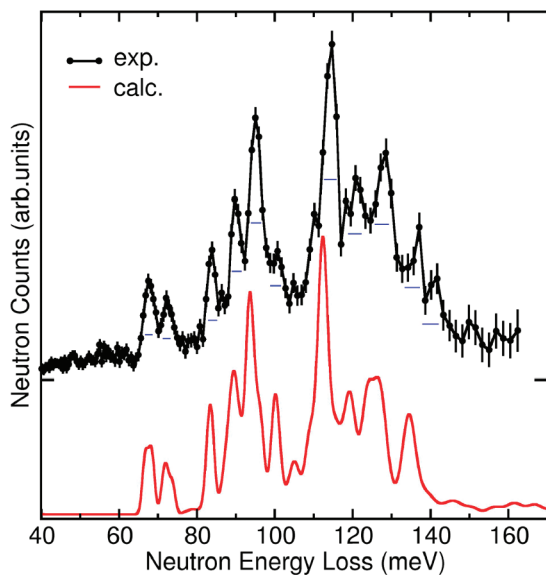


Figure 4. NVS spectrum (black, vertically offset for clarity) of $\text{Li}_2\text{B}_{12}\text{H}_{12}$ at 4 K compared with the calculated phonon DOS (red) of the optimized cubic structure. Horizontal bars denote the full-width-at-half-maximum instrumental resolution, and vertical bars represent $\pm 1\sigma$.

density functional theory (DFT) using a Vanderbilt-type ultrasoft potential with Perdew–Burke–Ernzerhof exchange correlation. Structural optimizations were performed with respect to atomic positions with lattice parameters fixed at the experimental values. The room-temperature structure from XRD data was numerically relaxed at 0 K. The optimized structure was close to that experimentally observed, suggesting that there is no structural phase transition between 0 K and room temperature. Differential scanning calorimetry showed no evidence of a phase transition down to 183 K.

The phonon DOS was calculated with the optimized structure using the supercell method with finite displacements^{10,11} and was in good agreement (see Figure 4 and Table 1) with the 4 K neutron vibrational spectrum for $\text{Li}_2\text{B}_{12}\text{H}_{12}$ measured using the BT-4 filter analyzer neutron spectrometer¹² at the NIST Center for Neutron Research. Spectral features are dominated by the various internal

Table 1. Fractional Coordinates of Anhydrous $\text{Li}_2\text{B}_{12}\text{H}_{12}$ from Powder XRD and DFT Relaxation^a

atom (Wyckoff)	XRD			DFT		
	<i>x</i>	<i>y</i>	<i>z</i>	<i>x</i>	<i>y</i>	<i>z</i>
Li1 (8c)	0.6400	0.6400	0.6400	0.6462	0.6462	0.6462
B1 (24d)	−0.0913	−0.0910	0.1236	−0.0903	−0.0885	0.1215
B2 (24d)	−0.0360	−0.0389	−0.1706	−0.0370	−0.0379	−0.1688
H1 (24d)	−0.1556	−0.1552	0.2107	−0.1519	−0.1515	0.2106
H2 (24d)	−0.0613	−0.0663	−0.2907	−0.0611	−0.0637	−0.2895

^a The lattice parameter was set to the experimental value. Cubic, space group $P\bar{a}3$, $a = 9.5771(2)$ Å, $V = 878.43(6)$ Å³, $Z = 4$.

vibrational modes of the $\text{B}_{12}\text{H}_{12}^{2-}$ anions involving hydrogen displacements. Prior NVS measurements¹³ of $\text{Cs}_2\text{B}_{12}\text{H}_{12}$ indicated that the phonon DOS is indeed sensitive to the structural details of the $\text{B}_{12}\text{H}_{12}^{2-}$ lattice arrangements and, as such, can facilitate structure identification. Thus, the observed phonon DOS is additional experimental evidence supporting the refined $\text{Li}_2\text{B}_{12}\text{H}_{12}$ structure.

In summary, the crystal structure of $\text{Li}_2\text{B}_{12}\text{H}_{12}$, a possible intermediate compound in the dehydrogenation of LiBH_4 , has been determined by XRD and corroborated by a combination of NVS and first-principles calculations. Such information is crucial for understanding, on a fundamental level, the role that $\text{Li}_2\text{B}_{12}\text{H}_{12}$ plays along the decomposition pathway of LiBH_4 to release hydrogen as well as its impact on LiBH_4 regeneration. Solid-state NMR, NVS, and Raman spectroscopy studies are in progress to ascertain more thoroughly the formation and reactions of $\text{Li}_2\text{B}_{12}\text{H}_{12}$.

Acknowledgment. The authors thank Drs. Craig M. Brown and John J. Rush for useful discussions, as well as Joseph W. Reiter and Dr. Chul Kim for their contributions to the experiments. This work was supported by the DOE through Awards DE-AI-01-05EE11104 and DE-AI-01-05EE11105 and was partially performed at the Jet Propulsion Laboratory, which is operated by the California Institute of Technology under a contract with NASA.

Supporting Information Available: Crystallographic data in CIF format, equipment details, a crystallographic data table, and information concerning structure solution and computation. This material is available free of charge via the Internet at <http://pubs.acs.org>.

IC801345H

(10) Kresse, G.; Furthmüller, J.; Hafner, J. *Europhys. Lett.* **1995**, *32*, 729.

(11) Yildirim, T. *Chem. Phys.* **2000**, *261*, 205.

(12) Udovic, T. J.; Neumann, D. A.; Leão, J.; Brown, C. M. *Nucl. Instrum. Methods A* **2004**, *517*, 189.

(13) Allis, D. G.; Hudson, B. S. *J. Phys. Chem. A* **2006**, *110*, 3744.